63 4-2 **TECHNICAL REPORT**

STABILITY OF THIN TORISPHERICAL SHELLS UNDER UNIFORM INTERNAL PRESSURE

by

JOHN MESCALL

METALS AND CERAMICS RESEARCH LABORATORIES

U. S. ARMY MATERIALS RESEARCH AGENCY

JUNE 1963   WATERTOWN 72, M

The findings in this report are not to be construed
as an official Department of the Army position.

STABILITY OF THIN TORISPHERICAL SHELLS UNDER UNIFORM INTERNAL PRESSURE

Technical Report AMRA TR 63-06

by

John Mescall

June 1963

STABILITY OF THIN TORISPHERICAL SHELLS UNDER UNIFORM INTERNAL PRESSURE

Technical Report AMRA TR 63-06
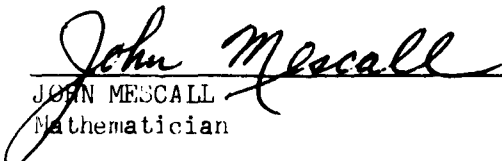
by

John Mescall

June 1963

U.S. ARMY MATERIALS RESEARCH AGENCY

TITLE

STABILITY OF THIN TORISPHERICAL SHELLS UNDER UNIFORM INTERNAL PRESSURE

ABSTRACT

The stability of the toroidal portion of a torispherical shell under internal pressure is considered from the point of view of the linear buckling theory. A detailed stress analysis of the prebuckled shell is made employing asymptotic integration. The change in potential energy of the shell is then minimized using a Rayleigh-Ritz procedure for actual computation of the critical pressure. Numerical results reveal that elastic buckling may occur for very thin shells whose material has a relatively high value of the ratio of yield stress to elastic modulus.

JOHN MESCALL
Mathematician

APPROVED:

E. N. HEGGE
Acting Director
Metals and Ceramics Research Laboratories

CONTENTS

SYMBOLS

α, β	coordinates of middle surface of shell
z	coordinate normal to middle surface of shell
A, B	Lamé coefficients associated with α, β
R_1, R_2	principal radii of curvature
u, v, w	displacements in the α, β, z directions
u_1, v_1, w_1	additional displacements in the meridional, circumferential, and normal directions after buckling
$\epsilon_\alpha, \epsilon_\beta, \epsilon_{\alpha\beta}$	strains at any point in the shell
$\sigma_\alpha, \sigma_\beta, \sigma_{\alpha\beta}$	stresses at any point in the shell
U	strain energy of thin shell
$\hat{\imath}, \varkappa$	middle surface strains and curvature changes in a thin shell
$\omega_\alpha, \omega_\beta$	angle of rotation of normal to middle surface about tangent to lines β = constant, α = constant
φ, θ	coordinates in meridional, circumferential direction on toroidal middle surface
b	radius of cross section of torus
a	distance from center line to center of toroidal cross section
r	$r = a + b \sin \varphi$, horizontal distance from center line to point on toroidal middle surface
λ	$\lambda = b/a$
$\bar{\lambda}$	$\bar{\lambda} = \dfrac{2\pi}{\pi - 2\varphi_0}$
h	shell thickness
E	Young's modulus of elasticity
ν	Poisson's ratio
D	flexural stiffness of torus: $\left[D = \dfrac{Eh^3}{12(1 - \nu2)} \right]$

p   applied pressure

p_{cr} critical pressure

n   wave number defining number of circumferential buckles in torus

$N_{\varphi_o}, N_{\theta_o}$ middle surface stress resultants prior to buckling

$M_{\varphi_o}, M_{\theta_o}$ middle surface stress couples prior to buckling

INTRODUCTION

Torispherical shells are frequently employed as end closures for cylindrical shells both in missile design and in a wide variety of industrial-type pressure vessels. Such shells generally consist of a shallow spherical cap joined to a toroidal segment, joined in turn to a cylindrical shell. This combined shell is then subjected to internal pressure. It was known[1] that large, compressive hoop stresses were developed in the torus, and that for very thin shells, elastic buckling was a distinct possibility. For shells whose thickness is heavy enough to avoid buckling, but which may still be rather thin compared to the toroidal radius, plastic deformation may occur. This has been examined in detail by Drucker and Shield.[2,3] However, the elastic stability of torispherical shells was not considered a matter for concern until, recently, such a shell was actually observed to buckle under internal pressure. (See Figure 1.) The problem is an interesting one, since the prebuckling state of stress in such a shell is not a simple one. The membrane state, often employed to estimate prebuckling stresses, would actually predict a state of tension in the torus. Consequently a thorough stress analysis of the shell prior to the onset of instability must be made. This stress analysis is also useful (and necessary) in ascertaining the dividing line between those configurations which are likely to buckle and those which are likely to undergo plastic deformation.

In this report, prebuckling stresses in a shell of the type shown in Figure 2, subjected to internal pressure, were determined by asymptotic integration techniques, with special attention being devoted to the particular solution. The vertical support on the cylinder was assumed to be sufficiently far removed from the junction of the torus that its specific form had little influence on the toroidal stresses. These results were then incorporated into the stability equations for the toroidal segment, and numerical results were obtained by applying a Rayleigh-Ritz approach to an appropriate potential energy expression. Since no prior theoretical results appear to be available, an experimental investigation of the same problem was undertaken simultaneously. The results of the two investigations compare favorably. Finally, a somewhat simplified stability criterion is proposed which provides results of essentially the same degree of accuracy, at a considerable saving in effort.

ANALYSIS OF THE ELASTIC STABILITY OF THIN TORISPHERICAL SHELLS
UNDER UNIFORM INTERNAL PRESSURE

Theoretical Background

Equations governing both the equilibrium and the stability of a thin elastic shell may be obtained in the following manner.[4],[5] Beginning with an appropriate set of strain-displacement relations and a stress-strain law, one forms the strain energy integral associated with the thin shell under consideration. For a homogeneous isotropic thin shell this may be expressed as

$$U = \frac{1}{2} \iiint \left[\sigma_\alpha \epsilon_\alpha + \sigma_\beta \epsilon_\beta + \sigma_{\alpha\beta} \epsilon_{\alpha B} \right] AB \, d\alpha \, d\beta \, dz \qquad (1)$$

Next, the principle of virtual work and the principle of stationary potential energy are applied. In this connection, consider a shell in a state of equilibrium characterized by displacements u_0, v_0, w_0. This state is said to be one of "neutral" equilibrium if there exists an adjacent equilibrium state differing from the first by an infinitesimal variation in the quantities characterizing that state. We therefore consider an alternate equilibrium state characterized by displacements

$$u = u_0 + \eta u_1 \qquad v = v_0 + \eta v_1 \qquad w = w_0 + \eta w_1 \qquad (2)$$

where η is an infinitesimal, independent of α, β.

The strain energy associated with this second state becomes

$$U = U_0 + \eta U_1 + \eta^2 U_2 . \qquad (3)$$

The principle of stationary potential energy implies that for the second state to be one of equilibrium,

$$\delta U + \delta V = 0, \qquad (4)$$

where δV is the negative work done by external loads due to a variation in displacements. Considering only variations in u_1, v_1, w_1, we have:

$$\delta U_1 + \delta V_1 + \eta(\delta U_2 + \delta V_2) = 0. \qquad (5)$$

But, since the first state was assumed to be an equilibrium state, the principle of virtual displacements implies that

$$\delta U_1 + \delta V_1 = 0. \qquad (6)$$

Hence the condition that the first equilibrium state be unstable is that

$$\delta U_2 + \delta V_2 = 0. \qquad (7)$$

To summarize, equation 6 yields equations governing the equilibrium of a state described by displacements u_0, v_0, w_0, while equation 7 yields equations governing the stability of this state. This general

statement of the problem is valid for both large and small deflections. Thus, depending upon the generality of the strain-displacement relations and the stress-strain laws assumed, a variety of theories is possible. Kempner[5] delineates several of these in considerable detail and with attendant clarity.

Toroidal Geometry and Strain-Displacement Relations

We consider the coordinate system shown in Figure 2 with φ, θ the middle surface coordinates in the meridional and circumferential directions and z normal to both, positive when directed inward. The principal radii of curvature R_1, R_2 are given by $R_1 = b$ and $R_2 \sin \varphi = a + b \sin \varphi = r$. The so-called Lamé coefficients for this system are $A_1 = b$ and $A_2 = R_2 \sin \varphi = r$. With this information it is a simple matter to obtain from Reference 4 or 5 (with obvious changes in notation) the following strain-displacement relations, valid for small strains but large rotations:

$$\varepsilon_\varphi = \ell_\varphi + \frac{1}{2}(\omega_\theta{}^2)$$

$$\varepsilon_\theta = \ell_\theta + \frac{1}{2}(\omega_\varphi{}^2)$$

$$\varepsilon_{\varphi\theta} = \ell_{\varphi\theta} - \omega_\varphi \omega_\theta \qquad (8a)$$

where

$$\ell_\varphi = \hat{\ell}_\varphi - z\varkappa_\varphi \qquad \ell_\theta = \hat{\ell}_\theta - z\varkappa_\theta$$

$$\ell_{\varphi\theta} = \hat{\ell}_{\varphi\theta} - z\varkappa_{\varphi\theta} \qquad (8b)$$

and

$$\hat{\ell}_\varphi = \frac{1}{b}(u,_\varphi - w) \qquad \hat{\ell}_\theta = \frac{1}{r}(v,_\theta + u \cos \varphi - w \sin\varphi)$$

$$\hat{\ell}_{\varphi\theta} = \frac{1}{b}(v,_\varphi) + \frac{1}{r}(u,_\theta - v \cos \varphi) \qquad (8c)$$

$$\chi_\varphi = -\frac{1}{b}(\omega_\theta)_{,\varphi} \qquad \chi_\theta = \frac{1}{r}(\omega_\varphi)_{,\theta} - \frac{\cos\varphi}{r}(\omega_\theta)$$

$$\chi_{\varphi\theta} = \frac{r}{b}\left(\frac{\omega_\varphi}{r}\right)_{,\varphi} - \frac{1}{r}(\omega_\theta)_{,\theta} \qquad (8d)$$

$$\omega_\varphi = \frac{1}{r}(w_{,\theta} + v\sin\varphi) \qquad \omega_\theta = -\frac{1}{b}(w_{,\varphi} + u) \qquad (8e)$$

In obtaining these relations, in addition to the underlying assumptions of thinness of the shell and validity of Kirchhoff's hypothesis, we have made the further assumptions that components of strain and rotation are small compared to unity, and in addition, strains are small compared to rotations, i.e., $\epsilon = O(\ell) = O(\omega^2) \ll 1$. Further, we have assumed that ω_z, the component of rotation in the plane of the middle surface of the shell is much smaller than the other two components, ω_φ and ω_θ. Finally, it is possible to effect a considerable saving in algebra with a minimal expense of accuracy by neglecting in ω_φ and ω_θ the contribution of the u,v terms. This may be justified on an order of magnitude estimate of the terms involved, or by examination of the effect of this approximation on numerical results. The latter reinforces the former. This approximation results in what is sometimes referred to as a Donnell-type theory. In what follows, then, we take,

$$\omega_\varphi = \frac{1}{r}(w_{,\theta}) \qquad \omega_\theta = -\frac{1}{b}(w_{,\varphi}). \qquad (8f)$$

With a stress-strain law assumed in the form

$$\sigma_\varphi = \frac{E}{1-v^2}(\epsilon_\varphi + v\epsilon_\theta) \qquad \sigma_\theta = \frac{E}{1-v^2}(\epsilon_\theta + v\epsilon_\varphi)$$

$$\sigma_{\varphi\theta} = \frac{E}{2(1+v)}\epsilon_{\varphi\theta} \qquad (9)$$

the strain energy of the shell may be written out in detail, as well as the quantities U_1 and U_2, sometimes referred to as the first and second variation of the strain energy. Specifically,

$$U_1 = \iiint (\sigma_{\varphi_0}\epsilon_{\varphi_1} + \sigma_{\theta_0}\epsilon_{\theta_1} + \sigma_{\varphi\theta_0}\epsilon_{\varphi\theta_1})brd\omega d\theta dz \qquad (10)$$

- 6 -

$$U_2 = \frac{1}{2} \iiint (\sigma_{\varphi_1} e_{\varphi_1} + \sigma_{\theta_1} e_{\theta_1} + \sigma_{\varphi\theta_1} e_{\varphi\theta_1}$$

$$+ 2[\sigma_{\varphi_0} e_{\varphi_{11}} + \sigma_{\theta_0} e_{\theta_{11}} + \sigma_{\varphi\theta_0} e_{\varphi\theta_{11}}]) br \, d\varphi \, d\theta \, dz \qquad (11)$$

where

$$\epsilon_{\varphi_0} = \ell_{\varphi_0} + \frac{1}{2}(\omega_{\varphi_0})^2 \qquad \epsilon_{\theta_0} = \ell_{\theta_0} + \frac{1}{2}(\omega_{\theta_0})^2 \qquad \epsilon_{\varphi\theta_0} = \ell_{\varphi\theta_0} - \omega_{\varphi_0}\omega_{\theta_0}$$

$$\epsilon_{\varphi_1} = \ell_{\varphi_1} + \omega_{\theta_0}\omega_{\theta_1} \qquad \epsilon_{\theta_1} = \ell_{\theta_1} + \omega_{\theta_0}\omega_{\theta_1} \qquad \epsilon_{\varphi\theta_1} = \ell_{\varphi\theta_1} - \omega_{\varphi_0}\omega_{\theta_1}$$

$$- \omega_{\varphi_1}\omega_{\theta_0}$$

$$\epsilon_{\varphi_{11}} = \frac{1}{2}(\omega_{\theta_1})^2 \qquad \epsilon_{\theta_{11}} = \frac{1}{2}(\omega_{\varphi_1})^2 \qquad \epsilon_{\varphi\theta_{11}} = - \omega_{\varphi_1}\omega_{\theta_1} \qquad (12)$$

and where it is to be understood that the subscripted strain or rotation is to be evaluated in terms of the displacement of the same subscript. Finally, σ_φ, σ_θ and $\sigma_{\varphi\theta}$ are related to the appropriately subscripted strains according to equation 9.

Stability Criterion

Employing linearized strain-displacement relations, we may obtain from equation 6 the equilibrium equations governing the (rotationally symmetric) prebuckling state of stress in the shell. We prefer to solve these in a somewhat different formulation however, and omit their presentation here. Proceeding directly to the stability relations we observe first that the prebuckled state is one of small deflections, governed by the classical (linear) theory. As Novozhilov[4] points out, then, we are justified in simplifying the expression for U_2 by omitting the ω_0 terms in ϵ_{φ_1}, ϵ_{θ_1} and $\epsilon_{\varphi\theta_1}$. Upon integrating through the thickness, h, we may write

$$U_2 = \frac{Eh}{2(1-\nu^2)} \iint \left\{ \ell_{\varphi_1}^2 + \ell_{\theta_1}^2 + 2\nu \ell_{\varphi_1} \ell_{\theta_1} + \frac{1-\nu}{2}\ell_{\varphi\theta_1} \right\} br \, d\varphi \, d\theta$$

$$+ \frac{Eh^3}{24(1-\nu^2)} \iint \left\{ X_{\varphi_1}^2 + X_{\theta_1}^2 + 2\nu X_{\varphi_1} X_{\theta_1} + 2(1-\nu)X_{\varphi\theta_1}^2 \right\} br \, d\varphi \, d\theta$$

$$+ \frac{1}{2} \iint \left\{ N_{\varphi_0}(\omega_{\theta_1})^2 + N_{\theta_0}(\omega_{\varphi_1})^2 - 2N_{\varphi\theta_0}(\omega_{\varphi_1}\omega_{\theta_1}) \right\} br \, d\varphi \, d\theta \qquad (13)$$

- 7 -

where N_{φ_0}, N_{θ_0} are the stress resultants of the prebuckled shell, and due to rotational symmetry prior to buckling, $N_{\varphi\theta_0} = 0$.

The potential energy of the external force system, V_2, is equal to the product of the external load and the increase in volume enclosed by the shell. An approximate expression for V_2 for the toroidal shell segment under uniform internal pressure p is[6]

$$V_2 = \frac{p}{2} \iint \left\{ \frac{w}{b}(u_{,\varphi} - w) + \frac{w}{r}(v_{,\theta} + u\cos\varphi - w\sin\varphi) \right.$$
$$\left. - \frac{v^2\sin\varphi}{r} - \frac{u^2}{b} - uw_{,\varphi} - \frac{vw_{,\theta}}{r} \right\} brd\varphi d\theta. \qquad (14)$$

Stability is governed by the relation

$$\delta(U_2 + V_2) = 0. \qquad (15)$$

It is clear that solution of the differential equations governing the stability of the toroidal shell segment would be a formidable task even if the prebuckled state were a simple one. For this reason we employ a Rayleigh-Ritz approach and obtain an upper bound for the critical pressure. In this connection, guided somewhat by experimental observation of the buckled pattern in the toroidal segment, we choose the following set of displacements

$$u_1 = \bar{A} \, r^2 \cos \bar{\lambda} \, (\varphi - \varphi_0) \cos (n\theta)$$

$$v_1 = \bar{B} \, r^2 \sin \bar{\lambda} \, (\varphi - \varphi_0) \sin (n\theta)$$

$$w_1 = \bar{C} \, r^2 \sin \bar{\lambda} \, (\varphi - \varphi_0) \cos (n\theta) \qquad (16)$$

where n is the number of lobes in the circumferential direction and $\bar{A}$, $\bar{B}$, $\bar{C}$ are undetermined coefficients. The variations in u_1, v_1, w_1 are reduced to variations in $\bar{A}$, $\bar{B}$, $\bar{C}$. Inserting equation 16 into equation 15 and requiring that the resulting equation be satisfied for arbitrary values of $\delta\bar{A}$, $\delta\bar{B}$, $\delta\bar{C}$, we obtain a system of three linear homogeneous algebraic equations in $\bar{A}$, $\bar{B}$, $\bar{C}$, whose determinant set equal to zero yields an estimate of the critical pressure. Omitting details of intermediate algebra we may write

- 8 -

$$\frac{P_{cr}}{E} = \frac{h}{2(1-\nu^2)b}\left(\frac{N}{D}\right) \tag{17a}$$

where

$$N = 4a_{11}a_{22}a_{33} - a_{11}(a_{23})^2 - a_{12}^2 a_{33} + a_{12}a_{13}a_{23} - a_{22}a_{13}^2$$

$$D = 2a_{11}a_{23}b_{23} + a_{23}^2 b_{11} + a_{12}^2 b_{33} + 2a_{13}a_{22}b_{13} + a_{13}^2 b_{22}$$

$$- a_{12}(a_{23}b_{13} + a_{13}b_{23}) - 4a_{33}(a_{22}b_{11} + a_{11}b_{22})$$

$$-4a_{11}a_{22}b_{33} \tag{17b}$$

where:

$$a_{11} = (5 + 4\nu)\left(\frac{12*}{b^3}\right) - 2(2 + \nu)\,\bar{\lambda}\left(\frac{25*}{b^4}\right) + \bar{\lambda}^2\left(\frac{26*}{b^5}\right) + \frac{(1-\nu)n^2}{2}\left(\frac{11*}{b^3}\right)$$

$$a_{12} = n(1 + 5\nu)\left(\frac{17*}{b^3}\right) - 2\nu n\bar{\lambda}\left(\frac{20*}{b^3}\right) - n\bar{\lambda}(1-\nu)\left(\frac{21*}{b^4}\right)$$

$$a_{13} = -2(2 + \nu)\left(\frac{25*}{b^4}\right) + 2\bar{\lambda}\left(\frac{26*}{b^5}\right) - 2(1 + 2\nu)\left(\frac{18*}{b^3}\right) + 2\nu\bar{\lambda}\left(\frac{22*}{b^4}\right)$$

$$a_{22} = n^2\left(\frac{10*}{b^3}\right) + (1-\nu)\left(2\left(\frac{15*}{b^3}\right) + \bar{\lambda}\left(\frac{25*}{b^4}\right) + \frac{\bar{\lambda}^2}{2}\left(\frac{27*}{b^5}\right) - \frac{3}{2}\left(\frac{13*}{b^3}\right)\right)$$

$$a_{23} = -2n\left(\frac{19*}{b^3}\right) - 2\nu n\left(\frac{20*}{b^4}\right)$$

$$a_{33} = \left(\frac{26*}{b^5}\right) + \left(\frac{14*}{b^3}\right) + 2\nu\left(\frac{22*}{b^4}\right) + \frac{h^2}{12b^2}\left\{8(1+\nu)\left(\frac{5*}{b}\right) + 4\left(\frac{14*}{b^3}\right)\right.$$

$$+ \bar{\lambda}^2(17+8\nu)\left(\frac{12*}{b^3}\right) + \bar{\lambda}^4\left(\frac{26*}{b^5}\right) - 8(1+\nu)\left(\frac{7*}{b^2}\right) + 20\,\bar{\lambda}(1+\nu)\left(\frac{9*}{b^2}\right)$$

$$- 4\,\bar{\lambda}^2(1+\nu)\left(\frac{13*}{b^3}\right) - 4\bar{\lambda}(4+\nu)\left(\frac{18*}{b^3}\right) + 4\bar{\lambda}^2\left(\frac{22*}{b^4}\right) + n^4\left(\frac{1*}{b}\right)$$

$$+ 4\nu n^2\left(\frac{6*}{b^2}\right) - 2\bar{\lambda}^3(4+\nu)\left(\frac{25*}{b^4}\right) + 2\nu\bar{\lambda}^2 n^2\left(\frac{10*}{b^3}\right) - 2n^2(1+3\nu)\left(\frac{3*}{b}\right)$$

$$+ 2n^2\bar{\lambda}(1-6\nu)\left(\frac{8*}{b^3}\right) + 2n^2(1-\nu)\,\bar{\lambda}^2\left(\frac{11*}{b^3}\right)\right\}$$

$$b_{11} = -\frac{1}{2}\left(\frac{27*}{b^5}\right)$$

$$b_{13} = -\frac{1}{2}\left[\bar{\lambda}\left(\left(\frac{27*}{b^5}\right) + \left(\frac{26*}{b^5}\right)\right) - \left(\frac{25*}{b^4}\right)\right]$$

$$b_{22} = -\frac{1}{2}\left(\frac{22*}{b^4}\right)$$

$$b_{23} = n\left(\frac{20*}{b^4}\right)$$

$$b_{33} = -\frac{1}{2}\left(\frac{26*}{b^5}\right) - \frac{1}{2}\left(\frac{22*}{b^4}\right) + K_2 \frac{n^2 b}{2} + \frac{K_1}{2b} \qquad (17c)$$

where the quantities (1*), etc., are definite integrals of the form

$$(1*) = \int_{\varphi_0}^{\pi/2} r \sin^2 \bar{\lambda}(\varphi - \varphi_0) d\varphi,$$

and are listed in the Appendix. All these integrals may readily be evaluated explicitly in terms of trigonometric functions. Finally,

$$K_2 = \int_{\varphi_0}^{\pi/2} N_{\theta_0} r^3 \sin^2 \bar{\lambda}(\varphi - \varphi_0) d\varphi$$

$$K_1 = \int_{\varphi_0}^{\pi/2} N_{\varphi_0} r\left(2r\, r,_\varphi \sin \bar{\lambda}(\varphi - \varphi_0) + \bar{\lambda} r^2 \cos \bar{\lambda}(\varphi - \varphi_0)\right)^2 d\varphi. \qquad (18)$$

Prebuckled State of Stress

In U_2 we encounter the integrals

$$\frac{1}{2} \iint N_{\varphi_0}\left(\frac{w,_\varphi}{b}\right)^2 br d\varphi d\theta, \qquad \frac{1}{2} \iint N_{\theta_0}\left(\frac{w,_\theta}{r}\right)^2 br d\varphi d\theta \qquad (19)$$

which assess the contribution of the prebuckled state of stress to the strain energy of the buckled state. Since the shells under consideration are very thin, the asymptotic method of solution of Reissner's equations for symmetric deformation of shells of revolution is most appropriate.

Clark[7,8] has presented asymptotic representations for both the homogeneous and particular solutions for the toroidal shell. These were employed in the present investigation.

In this connection, it may be well to digress for a moment to discuss the particular integral for toroidal shells. Galletley[1] has given ample warning that the frequently employed practice of using the membrane solution as a particular solution to the nonhomogeneous thin shell equations is not valid in the case of the torus. His results of a numerical integration of the complete differential equations for just such a torispherical-cylindrical shell show a markedly different stress pattern when compared to a solution using the membrane state as a particular solution. However, when the first two terms of an asymptotic particular solution developed by Clark[8] are used in conjunction with the homogeneous asymptotic solution, the results agree remarkably well with Galletley's. (See Figure 3.) This agreement is obtained at a value of the asymptotic parameter ($\mu \doteq 15$) which is considerably smaller than the values assumed by the shells whose stability we wish to consider, and thus assures validity of application of the asymptotic method.

Very briefly, the prebuckling stresses may be written in terms of the two basic functions β and Ψ according to the relations:

$$N_{\varphi_0} = \frac{Eh^2}{rm}(\Psi \cos \varphi + \Omega \sin \varphi)$$

$$N_{\theta_0} = \frac{Eh^2}{mb}(\Psi_{,\varphi} + \frac{m}{Eh^2} rbp_H) \tag{20}$$

where

$$\beta = (1+\lambda\sin\varphi)^{-1/2} Q \{A_0 h_{1r} - B_0 h_{1i} + C_0 h_{2r} - D_0 h_{2i} + \mu^{-2/3}(\lambda/D)^{1/2} \cdot$$

$$\cdot [F_0 T_r - G_0 T_i] + (\mu Q^{\Phi})^{-1}(\lambda/D)^{1/2}[G_0 Q^{-3} - G(\varphi)]\}$$

$$\Psi = (1+\lambda\sin\varphi)^{-1/2} Q\{B_0 h_{1r} + A_0 h_{1i} + D_0 h_{2r} + C_0 h_{2i} + (\mu^{-2/3}(\lambda/D)^{1/2} \cdot$$

$$\cdot [F_0 T_i + G_0 T_r]) - (\mu Q^{\Phi})^{-1} (\lambda/D)^{1/2}[F_0 Q^{-3} - F(\varphi)]\} \tag{21}$$

and

$$\lambda = b/a, \quad \mu = \frac{mb^2}{ah}, \quad m = \sqrt{12(1-\nu^2)}, \quad y = \mu^{1/3}\left(\tfrac{3}{2}\omega\right)^{2/3},$$

$$\omega = \int_0^\varphi \left(\frac{\sin\varphi}{1+\lambda\sin\varphi}\right)^{1/2} d\varphi, \quad Q = \left(\tfrac{3}{2}\omega\right)^{1/6}(\omega,_\varphi)^{-1/2},$$

$$\Omega = \frac{m}{Eh^2} rV = -\frac{m}{Eh^2}\int rbp_V d\varphi, \quad F(\varphi) = \left(\frac{\mu mb}{Eh^2(1+\lambda\sin\varphi)}\right)^{1/2}(rV)\cos\varphi,$$

$$G(\varphi) = \left(\frac{1+\lambda\sin\varphi}{\lambda Eh}\right)^{1/2}\left\{\frac{b\cos\varphi}{r}\left(\nu + \frac{b\sin\varphi}{r}\right)(rV) - 2b^2 p\sin\varphi\cos\varphi\right.$$

$$\left. - bpr\cos\varphi\right\}, \quad F_0 \equiv F(\varphi_0) \quad G_0 \equiv G(\varphi_0), \tag{21a}$$

p_H and p_V are the horizontal and vertical components of applied pressure. In the above, h_{1r}, h_{1i}, h_{2r}, h_{2i} are the real and imaginary components of the modified Hankel functions of order one-third, of the first and second kind respectively. Their argument is understood to be (iy). T_r, T_i are the real and imaginary parts of a special function introduced by Clark, and satisfying

$$T'' - iy \, T(y) = 1. \tag{22}$$

A_0, B_0, C_0, D_0 are constants to be determined from the boundary conditions of the specific problem considered. In the present analysis, a shallow spherical segment was assumed joined to the torus at $\varphi = \varphi_0$, and a cylinder at $\varphi = \frac{\pi}{2}$. The vertical support on the cylinder was assumed to be sufficiently far removed from the junction of the torus that its specific form had little influence on the form of the toroidal stresses. N_{φ_0}, N_{θ_0}, M_{φ_0} and M_{θ_0} were evaluated along the length of the torus. A typical set of results is shown in Figure 4. The integration indicated in equation 18 was carried out numerically. When this is done for a specific choice of geometric parameters, p_{cr}/E remains a function of n. The minimum value of critical pressure was found by calculating p_{cr}/E over a range of n, subject to the condition that n be an integer.

Simplified Formula for Critical Pressure

The procedure outlined above was carried out initially using equation 17. It soon became apparent that certain terms could be

omitted without significantly affecting the numerical results, and at the same time affording considerable simplification of the relation for critical pressure. The validity of the approximation rests on the fact that the value of n found to minimize p_{cr}/E was always rather a large number compared to unity. This result is consistent with experimental observations of the buckling pattern. (See Figure 1.)

The simplified relation for critical pressure may be written:

$$\frac{P_{cr}}{E} = \frac{h}{2(1-\nu^2)b}\frac{\bar{N}}{D} \qquad (n \gg 1) \qquad (23a)$$

where

$$\bar{N} = 4\,\bar{a}_{11}\,\bar{a}_{22}\,\bar{a}_{33} - \bar{a}_{11}\,\bar{a}_{23}^2$$

$$D = \bar{b}_{33}(\bar{a}_{12}^2 - 4\,\bar{a}_{11}\,\bar{a}_{22}) \qquad (23b)$$

$$\bar{a}_{11} = \left(\frac{1-\nu}{2}\right) n^2 \left(\frac{11*}{b^3}\right)$$

$$\bar{a}_{12} = -n\,\bar{\lambda}\left(2\nu\left(\frac{20*}{b^3}\right) + (1-\nu)\left(\frac{21*}{b^4}\right)\right)$$

$$\bar{a}_{22} = n^2 \left(\frac{10*}{b^3}\right)$$

$$\bar{a}_{23} = -2n\left(\left(\frac{19*}{b^3}\right) + \nu\left(\frac{20*}{b^3}\right)\right)$$

$$\bar{a}_{33} = \left(\frac{14*}{b^3}\right) + \left(\frac{26*}{b^5}\right) + 2\nu\left(\frac{22*}{b^4}\right) + \frac{h^2 n^4}{12b^2}\left(\frac{1*}{b}\right)$$

$$\bar{b}_{33} = b_{33} = -\frac{1}{2}\left(\left(\frac{26*}{b^5}\right) + \left(\frac{22*}{b^4}\right)\right) + K_2\frac{n^2 b}{2} + \frac{K_1}{2b}$$

$$K_2 = \int_{\varphi_0}^{\pi/2} N_{\theta_0}\, r^3\, \sin^2 \bar{\lambda}(\varphi - \varphi_0)\,d\varphi$$

$$K_1 = \int_{\varphi_0}^{\pi/2} N_{\varphi_0} r\left(2rr_{,\varphi}\sin\bar{\lambda}(\varphi - \varphi_0) + \bar{\lambda}\,r^2(\cos\bar{\lambda}(\varphi - \varphi_0))\right)^2 d\varphi.$$
$$(23c)$$

- 13 -

Equation 23 is to be preferred over equation 17 for computational purposes when n is large. In all cases considered in this investigation, the value of n minimizing p_{cr} was greater than 40 and in most cases was greater than 60.

Numerical Results - Comparison With Experiment - Discussion

Computations of the critical pressure have been carried out thus far for a limited number of parameters. A typical set of numerical results is shown in Figure 5. The parameters in these curves correspond to those involved in an experimental program concerned with the same problem. In each numerical evaluation of the critical pressure, a stress analysis of the unbuckled shell was made, the parameters K_1 and K_2 determined, and then the stability criterion evaluated.

In the experimental program, scale models representative of those used in missile applications were tested. These models were made of poly-vinyl chloride, a material chosen among other reasons for its relatively high ratio of yield strength to elastic modulus. Some of the results of these tests are also shown in Figure 5. In the case of the thickest shells tested, ($h/b > .007$) the disagreement between theory and experiment increased significantly. The prebuckling stress analysis for these shells revealed that at pressure levels below the predicted buckling pressure, the difference in principal stresses in the shell near the junction of torus and spherical cap had exceeded the yield stress of the material. Since our analysis has assumed elastic behavior throughout, it would not be expected to apply to the experimental material in this range of the parameters.

The following experimental result may also be of some interest. An aluminum torispherical bulkhead was tested under internal pressure. The parameters involved were

$$\varphi_\sigma = 35° \quad a = 34.43" \quad b = 18.07" \quad h_{average} = .081" \quad E = 10^7 \quad \nu = .3.$$

Dimples began to appear in the toroidal section at about p = 25 psi. The pressure level was increased to 40 psi, and when the load was released the dimples remained. The theoretical buckling pressure for a shell of this material (see Figure 5) is 64 psi. However, the prebuckling state of stress reveals that in the vicinity of $\varphi = 45°$, the value of $\dfrac{\sigma_\varphi - \sigma_\theta}{p}$ on the inside and outside surfaces reaches a value of 1300 and

- 14 -

1015, respectively. Thus, for aluminum with a yield stress of 35,000 psi (as was the case in the test described) a value of p = 25 psi would produce stresses very close to yield.

The plastic models of this configuration, however, appeared to buckle elastically at 3.2 psi. (Theory predicts 2.9 psi.) This corresponds to an elastic buckling pressure of 70 psi for aluminum with $E = 10^7$. The stress level induced near 45° in the torus in the plastic models for p = 2.9 psi is in the vicinity of 3700 psi, which is below the yield stress of the plastic material used.

It is clear, then, that the phenomenon of elastic buckling of torispherical shells under internal pressure occurs only for very thin shells whose material has a relatively high value of the ratio of yield stress to elastic modulus. With the increasing role being played by such materials in space structures, it is believed that the analysis described in this report will assist the designer toward his objective of increased efficiency. Finally, it should be pointed out that the analysis may be applied to toriconical shells simply by replacing the spherical cap by a cone in determining the prebuckled state of stress.

Figure 1. EXPERIMENTAL SETUP
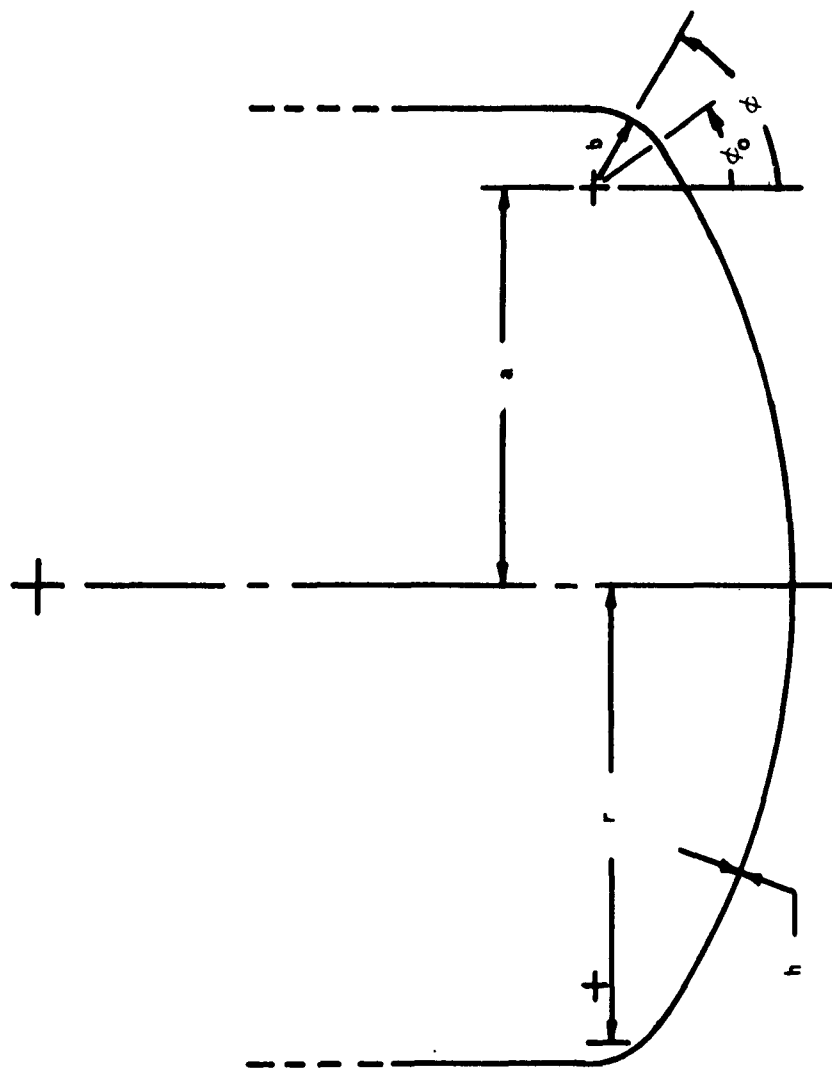
Figure 2. GEOMETRY OF TORISPHERICAL SHELL
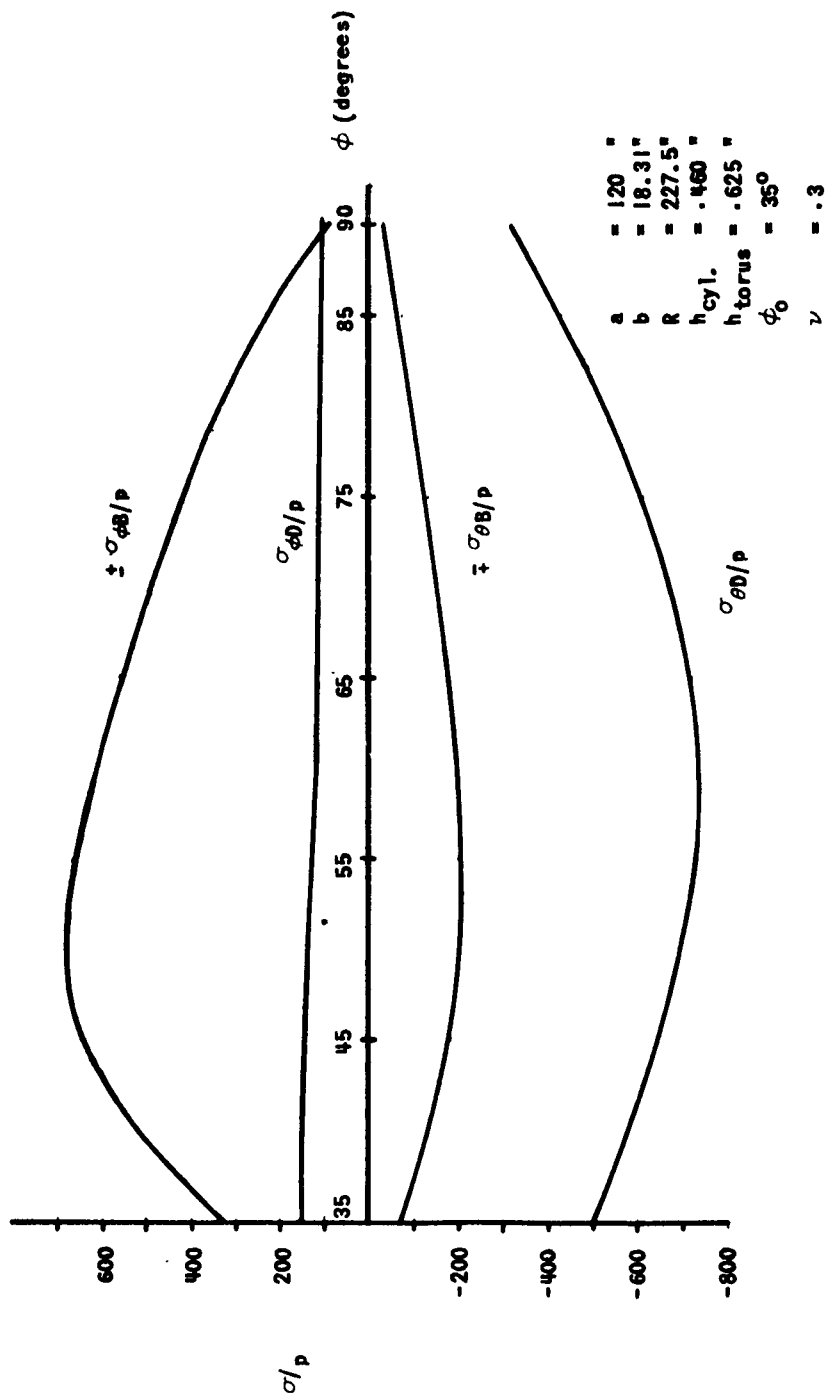
Figure 3. ASYMPTOTIC SOLUTION CORRESPONDING TO GALLETLEY'S (REFERENCE 1) NUMERICAL SOLUTION
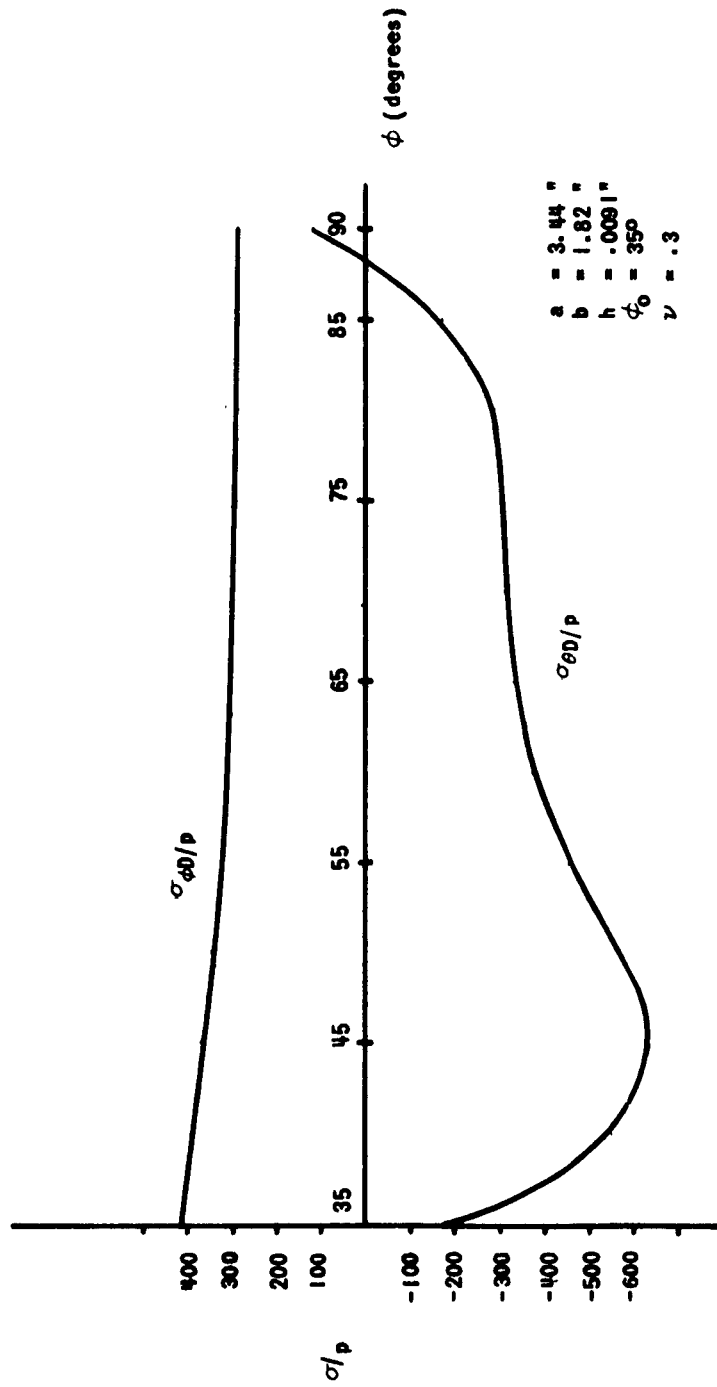
Figure 4. TYPICAL RESULTS OF PREBUCKLING STRESS ANALYSIS
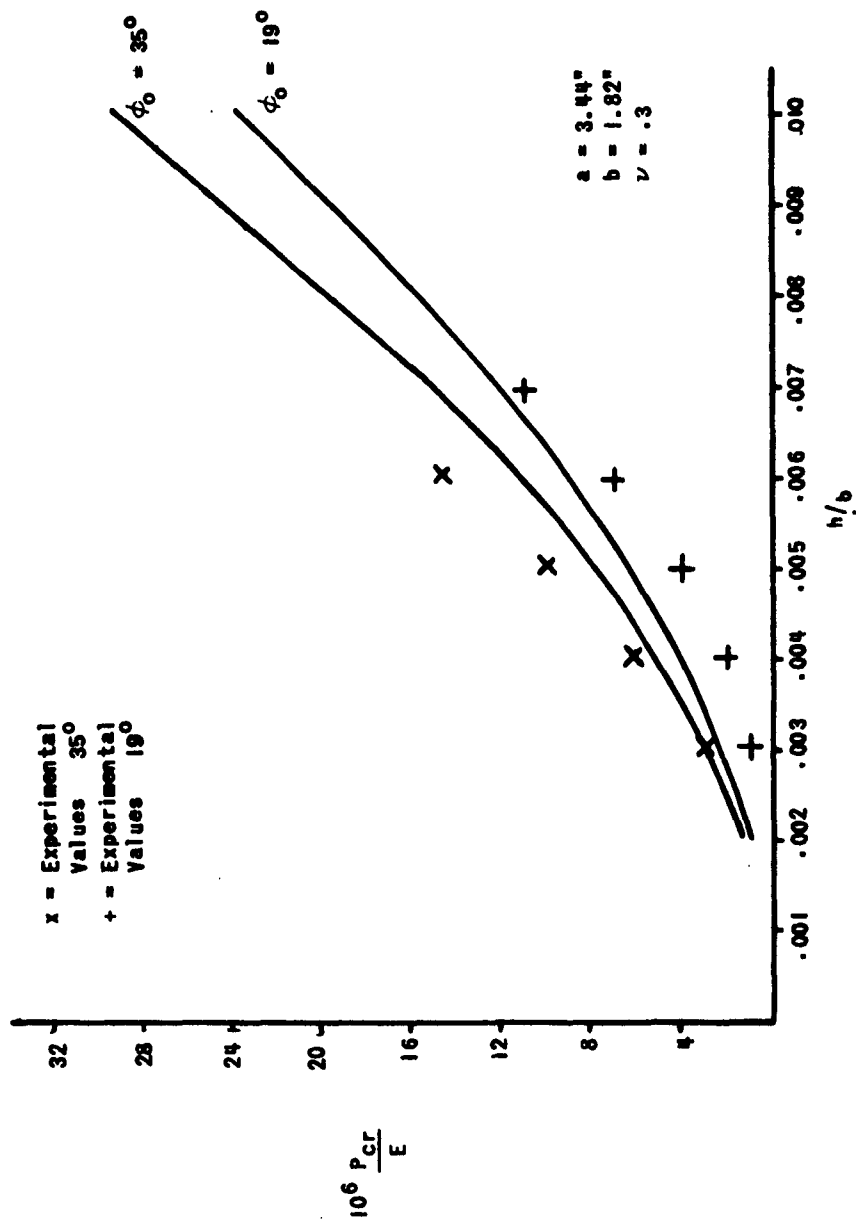
Figure 5. CRITICAL PRESSURE LEVELS

APPENDIX

The following definite integrals occur in the expression for critical pressure (equation 17 or 23). In each instance the limits of integration are from φ_0 to $\pi/2$. The variable r is given by $r = a + b \sin \varphi$. All integrals may be evaluated explicitly in terms of trigonometric functions.

$$1* = \int r \sin^2 \bar{\lambda}(\varphi - \varphi_0) d\varphi$$

$$2* = \int r \sin \varphi \cos^2 \varphi \sin^2 \bar{\lambda}(\varphi - \varphi_0) d\varphi$$

$$3* = \int r \cos^2 \varphi \sin^2 \bar{\lambda}(\varphi - \varphi_0) d\varphi$$

$$4* = \int r \cos^3 \varphi \sin^2 \bar{\lambda}(\varphi - \varphi_0) d\varphi$$

$$5* = \int r \cos^4 \varphi \sin^2 \bar{\lambda}(\varphi - \varphi_0) d\varphi$$

$$6* = \int r^2 \sin \varphi \sin^2 \bar{\lambda}(\varphi - \varphi_0) d\varphi$$

$$7* = \int r^2 \sin \varphi \cos^2 \varphi \sin^2 \bar{\lambda}(\varphi - \varphi_0) d\varphi$$

$$8* = \int r^2 \cos \varphi \sin \bar{\lambda}(\varphi - \varphi_0) \cos \bar{\lambda}(\varphi - \varphi_0) d\varphi$$

$$9* = \int r^2 \cos^3 \varphi \sin \bar{\lambda}(\varphi - \varphi_0) \cos \bar{\lambda}(\varphi - \varphi_0) d\varphi$$

$$10* = \int r^3 \sin^2 \bar{\lambda}(\varphi - \varphi_0) d\varphi$$

$$11* = \int r^3 \cos^2 \bar{\lambda}(\varphi - \varphi_0) d\varphi$$

$$12* = \int r^3 \cos^2 \varphi \cos^2 \bar{\lambda}(\varphi - \varphi_0) d\varphi$$

$$13* = \int r^3 \cos^2 \varphi \sin^2 \bar{\lambda}(\varphi - \varphi_0) d\varphi$$

$$14* = \int r^3 \sin^2 \varphi \sin^2 \bar{\lambda}(\varphi - \varphi_0) d\varphi$$

$$15* = \int r^3 \cos^2 \varphi \sin^2 \bar{\lambda}(\varphi-\varphi_0)d\varphi$$

$$16* = \int r^3 \cos \varphi \sin^2 \bar{\lambda}(\varphi-\varphi_0)d\varphi$$

$$17* = \int r^3 \cos \varphi \sin \lambda(\varphi-\varphi_0) \cos \bar{\lambda}(\varphi-\varphi_0)d\varphi$$

$$18* = \int r^3 \sin \varphi \cos \varphi \sin \bar{\lambda}(\varphi-\varphi_0) \cos \bar{\lambda}(\varphi-\varphi_0)d\varphi$$

$$19* = \int r^3 \sin \varphi \sin^2 \bar{\lambda}(\varphi-\varphi_0)d\varphi$$

$$20* = \int r^4 \sin^2 \bar{\lambda}(\varphi-\varphi_0)d\varphi$$

$$21* = \int r^4 \cos^2 \bar{\lambda}(\varphi-\varphi_0)d\varphi$$

$$22* = \int r^4 \sin \varphi \sin^2 \bar{\lambda}(\varphi-\varphi_0)d\varphi$$

$$23* = \int r^4 \sin \varphi \cos^2 \bar{\lambda}(\varphi-\varphi_0)d\varphi$$

$$24* = \int r^4 \cos^2 \varphi \cos^2 \bar{\lambda}(\varphi-\varphi_0)d\varphi$$

$$25* = \int r^4 \cos \varphi \sin \bar{\lambda}(\varphi-\varphi_0) \cos \bar{\lambda}(\varphi-\varphi_0)d\varphi$$

$$26* = \int r^5 \sin^2 \bar{\lambda}(\varphi-\varphi_0)d\varphi$$

$$27* = \int r^5 \cos^2 \bar{\lambda}(\varphi-\varphi_0)d\varphi$$

REFERENCES

1. GALLETLEY, G. D. *Torispherical Shells - a Caution to Designers.* Journal of Engineering for Industry, Transactions, American Society of Mechanical Engineers, v. 81, Series B, 1959, p. 51-62.

2. DRUCKER, D. C., and SHIELD, R. T. *Limit Analysis of Symmetrically Loaded Thin Shells of Revolution.* Journal of Applied Mechanics, Transactions, American Society of Mechanical Engineers, v. 81, Series E, 1959, p. 61-68.

3. SHIELD, R. T., and DRUCKER, D. C. *Design of Thin-Walled Torispherical and Toriconical Pressure-Vessel Heads.* Journal of Applied Mechanics, Transactions, American Society of Mechanical Engineers, v. 83, Series E, 1961, p. 292-297.

4. NOVOZHILOV, V. V. *Foundations of the Nonlinear Theory of Elasticity.* Graylock Press, Rochester, N.Y., 1953.

5. KEMPNER, J. *Unified Thin Shell Theory; Part I of A Symposium on the Mechanics of Plates and Shells for Industry Research Associates.* Polytechnic Institute of Brooklyn, March 9-11, 1960.

6. ALFUTOV, N. A. (Moscow). *On the Analysis of Shell Stability by the Energy Method.* Translated by M. 1. Yarymovych, Columbia University. Avco R & D, Translation, May 21, 1958.

7. CLARK, R. A. *On the Theory of Thin Elastic Toroidal Shells.* Journal of Mathematics and Physics, v. 29, 1950, p. 146-178.

8. CLARK, R. A. *Asymptotic Solutions of Toroidal Shell Problems.* Quarterly of Applied Mathematics, v. 16, 1958, 47-60.

Report No.: AMRA TR 03-06 June 1963   Title: Stability of Thin Torispherical Shells under Uniform Internal Pressure

No. of Copies	To
1	Advanced Research Projects Agency, The Pentagon, Washington 25, D.C.
10	Armed Services Technical Information Agency, Arlington Hall Station, Arlington 12, Virginia
1	Defense Metals Information Center, Battelle Memorial Institute, Columbus 1, Ohio
1	Commanding Officer, U. S. Army Research Office, Arlington Hall Station, Arlington 12, Virginia
	Commanding Officer, Army Research Office (Durham), Box CM, Duke Station, Durham, North Carolina
1	ATTN: Physics Division
	Commanding General, U. S. Army Materiel Command, Washington 25, D.C.
1	ATTN: AMCRD-RS, Research Division
1	AMCRD-RS, Scientific Deputy
1	AMCRD-RS-CM, Mr. J. Kaufman
1	AMCRD-RS-CM-M, Dr. P. Kosting
1	AMCRD-DE, Development Division
	Commanding General, U. S. Army Electronics Command, Fort Monmouth, New Jersey
1	ATTN: Institute for Fundamental Research
	Commanding General, U. S. Army Missile Command, Redstone Arsenal, Huntsville, Alabama
1	ATTN: AMSMI-RB, Redstone Scientific Information Center
1	Directorate of R&D
1	Chief Scientist, Dr. W. W. Carter
1	Dr. B. Steverding .
	Commanding General, U. S. Army Mobility Command, 28251 Van Dyke Avenue, Center Line, Michigan
1	ATTN: Physical Sciences Laboratory

No. of Copies	TO

Commanding General, U. S. Army Munitions Command, Dover, New Jersey
1   ATTN: Chief Scientist

Commanding General, Headquarters, U. S. Army Tank-Automotive Center, Detroit Arsenal, Center Line, Michigan
1   ATTN: SMOTA-RCM.1

Commanding General, U. S. Army Test and Evaluation Command, Aberdeen Proving Ground, Maryland
1   ATTN: AMSTE-LM, Technical Library

Commanding General, U. S. Army Transportation Research Command, Fort Eustis, Virginia
1   ATTN: Physical Science Division, Dr. G. D. Sands

Commanding General, U. S. Army Weapons Command, Rock Island, Illinois
1   ATTN: Chief Scientist

Commanding Officer, U. S. Army Ballistics Research Laboratories, Aberdeen Proving Ground, Maryland
1   ATTN: Dr. Coy Glass

Commanding Officer, U. S. Army Chemical Corps Nuclear Defense Laboratories, Army Chemical Center, Maryland
1   ATTN: Nuclear Physics Division

1   Commanding Officer, U. S. Army Engineer Research and Development Laboratories, Fort Belvoir, Virginia

Commanding Officer, U. S. Army Quartermaster Research and Engineering Laboratories, Natick, Massachusetts
1   ATTN: Pioneering Research Division, Dr. S. D. Bailey

Commanding Officer, Harry Diamond Laboratories, Washington 25, D.C.
1   ATTN: AMXDO-TIB

Commanding Officer, Frankford Arsenal, Bridge and Tacony Streets, Philadelphia 37, Pennsylvania
1   ATTN: Pitman-Dunn Laboratories
1   Research Institute

Commanding Officer, Picatinny Arsenal, Dover, New Jersey
1   ATTN: Feltman Research Laboratories
1   Technical Library

Commanding Officer, Rock Island Arsenal, Rock Island, Illinois
1   ATTN: 9320, Research and Development Division

No. of Copies	TO

1	Commanding Officer, Springfield Armory, Springfield 1, Massachusetts ATTN: SWESP-TX, Research and Development Division
1	Commanding Officer, Watervliet Arsenal, Watervliet, New York ATTN: Research Branch
1	Commander, Office of Naval Research, Department of the Navy, Washington 25, D. C.
1	Director, Navy Research Laboratories, Anacostia Station, Washington 25, D. C.
1	Commanding General, Air Force Cambridge Research Laboratories, Hanscom Field, Bedford, Massachusetts ATTN: Electronic Research Directorate
1 1	Commanding General, Air Force Materials Central, Wright-Patterson Air Force Base, Ohio ATTN: Physics Laboratory Aeronautical Research Laboratories
1	Commander, Office of Scientific Research, Air R&D Command, Temporary Building T, Washington 25, D. C.
1	U. S. Atomic Energy Commission, Washington 25, D. C. ATTN: Office of Technical Information
1	U. S. Atomic Energy Commission, Office of Technical Information Extension, P.O. Box 62, Oak Ridge, Tennessee
1	Director, George C. Marshall Space Flight Center, Huntsville, Alabama ATTN: M-S&M-M, Dr. W. Lucas
1	Director, Jet Propulsion Laboratory, California Institute of Technology, Pasadena 3, California ATTN: Dr. L. Jaffe
1	Director, Lewis Research Center, Cleveland Airport, Cleveland. Ohio
1	Director, National Bureau of Standards, Washington 25, D. C.
1	Director, Research Analysis Corporation, 6935 Arlington Road, Bethesda, Maryland

No. of Copies	TO

Commanding Officer, U. S. Army Materials Research Agency, Watertown 72, Massachusetts

5	ATTN: AMXMR-LXM, Technical Information Section
1	AMXMR-OPT
1	AMXMR, Dr. R. Beeuwkes, Jr.
1	Author

63 -- TOTAL COPIES DISTRIBUTED